FQXi
2010 Essay
Contest

Is Reality Digital or Analog ?

Hacking reality code

R. Aschheim[a]

[a]*Polytopics Research Institute, 8 villa Haussmann, 92130 Issy, France, raymond@aschheim.com*

January 30, 2011

Abstract

Can reality emerge from abstraction, from only information ? Can this information be self emergent? Can a structure be both the software and the hardware? Can it be ultimately simple, just equivalent to a set? Can symmetry spontaneously appear from pure mathematical consideration, from the most symmetric concept, a platonic "sixth element"? Would this symmetry be just structuring all the particles we know? Can all this be represented? Can standard physics be computed from this model? Eight questions: eight times yes. So this model is definitely DIGITAL, and is postulated to be reality.

I. INTRODUCTION

We want to understand our physical universe, at least a space-time hosting 3 families of fermions, and a few bosons, interacting through strong, weak, electro-magnetic and gravitation forces, verifying general relativity at large scale, and all the known symmetries of quantum physics at particle scale. We do not start with an underlying geometrical background space. At the beginning the structure has to be just a set, the set of subsets of cardinal 3, and designed as a trivalent graph, a purely discrete and informational structure not needing any previous background to exist. We demonstrate that such a structure has to fit standard physics. The underlying geometry has to be an F4 hyper-diamond lattice, designing a four-dimensional crystal, with super-nodes at centers of the D4 optimal sphere packing and densest regular lattice, linked to 24 neighbors at vertices of the sixth element, the 4D platonic icositetrachoron (or 24-cell), and 24 links to vertices of the dual figure, in the same lattice. From this exceptional self-duality emerges an 8D ultra-local structure with all 240 E8 roots characterizing particles, both fermions and bosons, in a non-associative manner, where triality, as a rotation, explains why there are 3 families of particles. We show how this 48-valent super-node is naturally built as a trivalent spin network topologically encoding 48 bits of information, where the maximal symmetry is the state of void, and an increasing number of defects (or bugs) encodes photons, bosons and fermions. General relativity emerges by using Loop Quantum Gravity on the model where, in Ashtekar variables, the frame-field and the connection are implicitly encoded by the local network topology, through an encoding we disclose here.

Our model is developed to provide a framework for digital physics [1]. It is a conceptual breakthrough in the definition of a space based on set theory [2]. We can compute gravitational field [3] from its metrics. Here we specify its formalism in information theory, and build foundation for applying Loop Quantum Gravity on it.

This model is a complex system on several levels, where the fundamental level is that of a trivalent graph.

The second level is the encoding of information in the topological graph structure.

The third is the encoding of local symmetries and algebraic properties.

The fourth is the emergence of a metrics, a dimensionality and a curvature of the assembly of sub-graphs, as super-nodes in a network of crystalline type.

It is possible to work at every level of this model by maintaining a good coherence. We optimize at a fundamental level the simplicity of the structure, while allowing the emergence of great complexity in the modeled system.

The hyperdiamond model is postulated to be reality because one metaphysical and mathematical reason -the

exceptional self-duality and dimensional unicity of the sixth element makes it the ultimate symmetry-, and one physical and scientific reason -this symmetry gives birth to exactly the particles observed in the reality, with all their symmetries, and the "falsifiable" prediction of some new bosons.

The same approach can be practiced while using other lattices (than F4), to build toy models for pedagogical reason. This family of models is designed to provide a framework for a new theory of everything, unifying in theoretical physics, the phenomena of quantum physics and our knowledge of the standard model with gravity and the conception of a space according to general relativity. Whether if reality is digital or analog, our model is digital.

There is still debate, and this FQXi question may close it, whether the nature of the universe is discrete or continuous. Some even speculate that the reality is the alliance of two [4] *"Conjecture 1: At some energy level, space-time is the product of a continuous four-dimensional manifold times a discrete space F."*

Others postulate a discrete system (and possibly finite) is sufficient for the emergence of an apparent continuity, which is an approximation of the discrete.

The main result of the present work is the demonstration that a phenomenon hitherto treated as continuous course, emerges naturally in our discrete model: gravity. As it emerges from a simple graph, we call it "**graphitation**". A similar word game has already been used for an approach to quantum physics in a graph, called *"Quantum Graphity"* [5] [6]. But the approaches are different; physicists have built several discrete models, graphs or networks, to implement continuous physical equations, by keeping the current models in discrete format. These approaches are top-down, as they depart from known results, to find a consistent underlying structure.

Our approach is bottom up, starting with a simple model ultimately (in fact the level of set theory, the foundation of mathematics), and constructing according to a principle of economy, said *"Okham's razor principle"* [7] *(Rursus absque necessitate et utilitate est pluralitas fugienda)* [8] a layered model to the more complex reality..

II. GRAPHITATION, BOTTOM-UP APPROACH

In our bottom-up approach, we start with a trivalent undirected graph.

1.1. Construction

A **graphiton** model is a trivalent graph checking at least two properties: a quasi-invariance on a large scale (a large number of nodes in the graph, evenly spaced, are topologically equivalent if one neglects a small number of disturbances), a characterization of local geometry at small-scale by the presence of triangular loops encoding bit 1.

Graphiton, a basic element of our model, is simply a node with three ends, each connected to another graphiton.

So, while any totally trivalent graph is a blend of **graphitons**, for it to be a model, it must satisfy the properties of global quasi-invariance and local geometric encoding.

A **graphiton** model can be interpreted in different scales. We will distinguish four scales (see Figure 1).

Level 0 is the fundamental level, in which the model is a simple undirected trivalent graph, where any node or connection doesn't carry additional information.

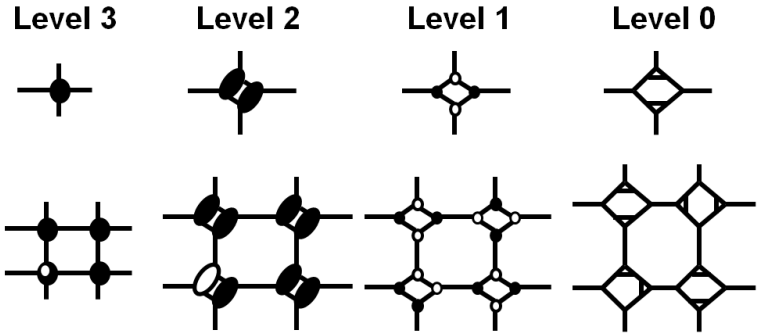

Fig. 1. Four-level view of a) a simple node, b) a sub-graph. At level 3 (supernode) the graph is not trivalent. At level 2 (differential bits) tetravalent bits appears. At level 1 (topological bits), nodes are added so the graph becomes trivalent, and nodes hold a bit. At level 0 (trivalent graph), 1-valued nodes are replaced by triangles. The structure exists only at level 0, but can be decoded at levels 1, 2 and 3.

Level 1 is obtained from level 0 by adding a binary property in each node; each node carries a bit, taking the value 0 or value 1.

The equivalence between Level 1, informed graph, and level 0, is ensured by the transformation T2 (see Figure 3) by Alexander [9], which replaces each node with a value of 1 at level 1 as a triangle consisting of three nodes at 0, and does not change the nodes on the value 0 to level 1.

If the graph is information homogeneous, id-est. contains as much bit 0 as bit 1 at level 1, while its equivalent in level 0 will double its number of nodes (and therefore connections).

Unless explicitly stated otherwise, we always work on **information homogeneous** graphs.

Our models have a natural encoding and regular, homogeneous information, which can be seen as physically optimum polarization for a certain Hamiltonian, defining a ground state of the system.

This system may be disrupted and contain additional information, at level 2, by inverting two narrow bits 0 and 1.

We show (see Figure 4) that this inversion is made only by means of Alexander's T1 transformations (see Figure 2), which provides a number of dynamic invariant systems, and indirectly, ownership of causal invariance discussed by Wolfram [10]. This T1 transformation is also refereed in literature as 2-2 Pachner move, or bistellar flip.

The concept of dynamic trivalent network (trinet) evolving by these moves (named "diags") was explored in [11].

The T1 transformation is intuitively the simplest, most realistic, most economic possible evolution of a trivalent graph. It applies to a connection between two nodes, and involves two other neighbors of each of these nodes. Of these 6 nodes forming the face of an H if the connection is in horizontal view, the T1 transformation rotates H 90 degrees. This can be done on a continuous basis through a transient state in which a tetravalent nodes 5 is at the center of an X shaped figure (Figure 2 When nodes 5 and 6 are merged).

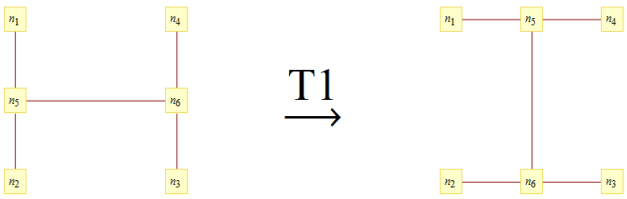

Fig. 2. Elementary move: T1 inversion

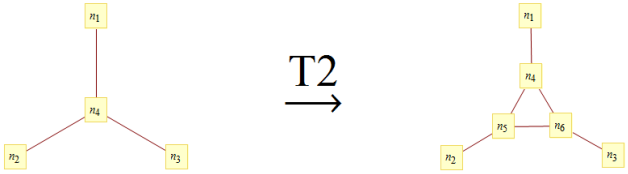

Fig. 3. Elementary move: T2 insertion

At each connection, we can apply two different transformations T1, according to one of the first neighboring node is found connected to a second neighbor node, or the other.

If the graph is locally planar, one T1 transformation retains planarity, and the other does not keep, thereby determining an implicit one that will be applied.

1.2. Disrupting

At level 1 (see Figure 1), a disturbance is the inversion of values 0 and 1 of two bits carried by two nodes, either neighbor (at distance 0), or narrow (at distance 1, separated by a node); thus giving a 1 value to the corresponding 'differential bit' at level 2. Differential here means inverted versus a polarized information background.

1─0 ↔0─1

1─1─0 ↔ 0─1─1, 1─0─0 ↔ 0─0─1 (figure 4)

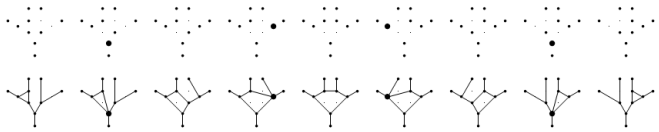

Fig. 4. Bit inversion 1─0─0 ↔ 0─0─1 as a sequence of four Alexander T1 moves (The transient four-valent X-state is enhanced by a bigger dot).

1.3. Dimension of the system as a space

The dimension of the graph depends on the chosen scale. We distinguish three levels:

Ultra-local dimension: around a node, a trivalent graph is of dimension 2 [12] considered the local restriction of a hexagonal lattice.

Local scale: within a super node, the structure is that of a binary tree whose dimension is infinite, because the number of neighbors at a distance r increases as 2^r, and therefore more quickly than r^d for any finite dimension d.

Global dimension: imposed by the regular system chosen (2 with a grid, 4 with hyperdiamond [13], n-1 with a simplex ...)

1.4. Global topology of space

Closure can imply a shift if a line does not meet itself after a tour, but a neighbor, like the non-commutative torus.

Closure may reverse the orientation, forming a Moebius strip, a Klein bottle, or other not oriented spaces [14].

1.5. Lattice regularity

- Regular lattice

We can apply our model to any regular lattice, like the square lattice, the checkerboard lattice, or even lattices in the A, D, E, F families.

We can further investigate applying it to quasi-regular lattices: Quasi-crystal or Penrose tiling (cf. [15]).

- Almost –regularity

We can expand the set of acceptable models to almost-regular lattice, defined as regular lattices admitting a number of irregularities $< n^{(d-1)}$ for a graph of n^d nodes and global dimension d.

- Local regularity

As a special case of almost-regularity, we can build models which physically correspond to the structure of natural crystals. They are admitting irregularities on the surfaces of dimension *d-1*; locally regular but globally isotropic. The space is broken into pieces of irregular crystals which themselves are regular but not parallel to each other.

It will then be useful to study the dynamic behavior to inter-crystalline walls.

From a mathematical point of view, the almost-regularity and local regularity are similar because they induce the same small number of irregularities with respect to the global regularity necessary.

1.6. Intrinsic space

The fundamental advantage of the **graphiton** model is its creation of intrinsic space. The system from the outside is a graph whose nodes do not coordinate in any space (unlike all previous approaches to discretization of physics). But thanks to the encoding of information in the topology of this graph, the model finds the characteristics necessary for a metric space, beyond the mere internal metrics of the graph, which alone would be insufficient. The **graphiton** model is an information system capable of emulating a space. And a rather rich area because it is Riemannian [16] and admits a local curvature, it can be Ricci-flat, where, in the absence of disturbance, any node at level 3 is topologically equivalent [3]. And most importantly, local disturbances linearly induce a curvature, then a tilt of geodesics at any point in space, forming a gravitational field. This field is attracted towards disturbances that are at its origin, and is additive; these are necessary conditions for a gravitational field reflecting the effect of mass disruption. So this space is quite a natural framework for a theory of general relativity. But if space is locally anisotropic as directions are marked by the regular network, the gravitational induced field remains isotropic and not

focused only along the directions of the network. Thus a movement in the network in response to the gravitational field can follow any direction not subject to the directions of the network.

1.7. Space as a network

The general idea that the ultimate nature of space is a trivalent graph and some topological characteristics of this graph encode a mass effect, with a result on the curvature and the possibility of calculating a Ricci curvature and the Einstein field equation [16] was developed by Wolfram in [10].

The fundamental contribution we make to this concept and which allows an effective implementation is to effectively place a layer of information in the graph at level 1, associated with the regular structure at level 2. This layer allows information to move intrinsically within the graph at a selected distance in both directions (2 directions for each dimension), and calculate the gravitational field and the Ricci tensor [16].

In the most random graph models proposed by Wolfram, these calculations were impossible and the notions of Ricci tensor couldn't be defined clearly. In other discrete models based on regular arrays, the authors postulated the existence of all space, locally Euclidean and continuous extrinsic to their model, in which they plunged their model to a metric and coordinates. What is less well founded and elegant than the concept of Wolfram!

We have therefore in the extreme elegance of the model suggested by Wolfram, the only model of intrinsic system which does not need to be plunged into another space to be calculated. But we overcome its lack of metrics by imposing constraints of regularity and topological encoding of the local orientation.

III. MATHEMATICAL FORMALISM

We give a formal description of our **graphiton** model.

Definition 1: rank r binary tree

$$\mathbb{B}_r := \{\underset{k=0}{\overset{2^r-1}{\text{nodes}}}\{n_k\}, \text{links}\{(n_0,n_1)\cup\cup\underset{k=1}{\overset{2^{r-1}-1}{(n_k,n_{2k})}}\cup\cup\underset{k=1}{\overset{2^{r-1}-1}{(n_k,n_{2k+1})}}\}\} \quad (1)$$

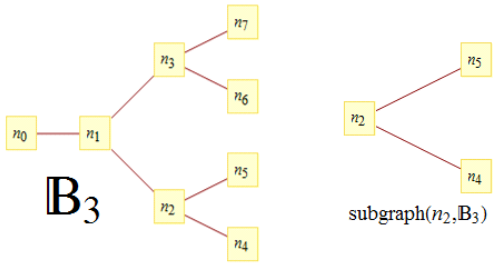

Fig. 5. Examples: a $\mathbb{B}_3$ graph (left), its subtree from $\boldsymbol{n_2}$(right)

Definition 2: descendants is a set of nodes descendants from one node

$$\text{descendants}(n_k \text{in} \mathbb{B}_r) := \{\begin{matrix}\text{if} k < 2^{r-1}: n_k \cup \text{descendants}(n_{2k} \text{in} \mathbb{B}_r) \cup \text{descendants}(n_{2k+1} \text{in} \mathbb{B}_r) \\ \text{else}: n_k\end{matrix} \quad (2)$$

Definition 3: subtree is the part of the tree emerging from a node (see Figure 5)

$$\text{subtree}(n_k \text{in} \mathbb{B}_r) := \mathbb{B}_r \cap \text{descendants}(n_k \text{in} \mathbb{B}_r) \quad (3)$$

Definition 4: an operator Ξ glues three binary trees (of the 4 subtrees) to build a triple-binary trivalent graph (see Figure 6)

$$\mathbb{T}_r = \Xi(\mathbb{B}_r) \text{by}\{\begin{matrix}\text{removenodes}\{n_3, \text{descendants}(n_6)\} \text{and their links} \\ \text{addlinks}(n_2,n_0)(n_0,n_5)(n_1,n_7), \text{removelink}(n_2,n_5)\end{matrix} \quad (4)$$

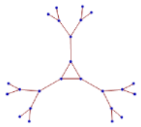

Fig. 6. 24-nodes module $\mathbb{T}_5 = \boldsymbol{\Xi}(\mathbb{B}_5)$, rank 5, with 12 leaves

Definition 5: we define the binary decomposition of an integer

$$\beta(K) := \{b_{i,K}\} \in \{0,1\}^{\lfloor 1+\frac{\mathrm{Log}K}{\mathrm{Log}2} \rfloor} \; / K = \sum_{i=0}^{\lfloor \frac{\mathrm{Log}K}{\mathrm{Log}2} \rfloor} b_{i,K} 2^i \quad (5)$$

Definition 6: we define the frequency of a quaternion

$$\omega(x) := \frac{1}{\pi}\mathrm{ArcCos}(\mathrm{Re}(x)) \quad (6)$$

Definition 7: we define the logarithm of a quaternion from its frequency

$$\log(x) = \log(\; / x \; /) + \pi\omega(x)\frac{\mathrm{Im}(x)}{/\,\mathrm{Im}(x)\;/} \quad (7)$$

Definition 8: we define a family of r couples of a frequency and an imaginary direction

$$\Omega_r := \{\{\omega_k, u_k\} \; / k \in \mathbb{N} \cap [0, r[, \omega_k \in]0,1], u_k = \mathrm{Im}(u_k), \; / u_k \; / = 1\} \quad (8)$$

Definition 9: we define a series of increasing products

$$\forall K \in \mathbb{N} \cap [0, 2^r[, \zeta(K, \Omega_r) := \eta(\beta(K), \Omega_r) = \prod_{i=0}^{r-1} \exp(b_{r-1-i,K} 2\pi\omega_i u_i) \quad (9)$$

Definition 10: we define a sample family, for r=6

$$\Omega_6{}^{\dagger} := \{\{\tfrac{1}{3}, (\tfrac{\mathbb{i}+\mathbb{j}+\mathbb{k}}{\sqrt{3}})\}, \{\tfrac{1}{3}, (\tfrac{\mathbb{i}+\mathbb{j}+\mathbb{k}}{\sqrt{3}})\}, \{\tfrac{1}{6}, (\tfrac{\mathbb{i}+\mathbb{j}+\mathbb{k}}{\sqrt{3}})\}, \{\tfrac{1}{4}, (\tfrac{\mathbb{i}}{\sqrt{1}})\}, \{\tfrac{1}{4}, (\tfrac{\mathbb{j}}{\sqrt{1}})\}, \{\tfrac{1}{8}, (\tfrac{\mathbb{i}}{\sqrt{1}})\}\} \quad (10)$$

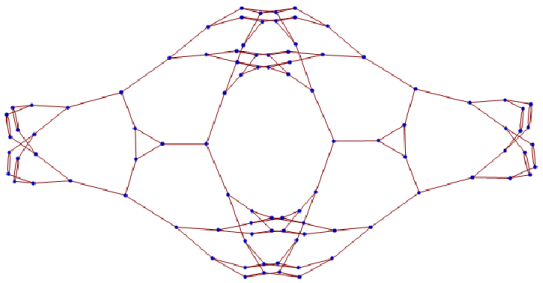

Fig. **7**. Level 1 view of simplest closed lattice of triple binary trees with $\boldsymbol{\Omega_6}^{\dagger}$ is made of 2 modules $\mathbb{T}$ [6] and has 144 connections and 96 nodes.

Definition 11: we define a unitary diagonal quaternion

$$\mathbb{u} := (\tfrac{\mathbb{i}+\mathbb{j}+\mathbb{k}}{\sqrt{3}}) \quad (11)$$

Definition 12: we define a suite of quaternions

$$\zeta(K, \Omega_6{}^{\dagger}) := ((((\exp(b_{5,K}\frac{2\pi}{3}\mathbb{u})\exp(b_{4,K}\frac{2\pi}{3}\mathbb{u}))\exp(b_{3,K}\frac{2\pi}{6}\mathbb{u}))$$
$$\exp(b_{2,K}\tfrac{2\pi}{4}\mathbb{i}))\exp(b_{1,K}\tfrac{2\pi}{4}\mathbb{j}))\exp(b_{0,K}\tfrac{2\pi}{8}\mathbb{i}) \quad (12)$$

Definition 13: a field $\mathbb{E}$ is defined at each node, having a quaternionic value computed using two functions ω and $\zeta$and one set of constants Ω_r

$$\forall K \in \mathbb{N} \cap [0, 2^{r+1}[, \forall n_k \in \mathrm{nodes}(\mathbb{B}_{r+1}),$$
$$\mathbb{E}(n_k) := \begin{cases} \mathrm{if} k < 2^r : \mathbb{E}(n_{2k}) \\ \mathrm{else}: \omega(\zeta(K-2^r, \Omega_r))\frac{\mathrm{Im}(\zeta(K-2^r,\Omega_r))}{/\,\mathrm{Im}(\zeta(K-2^r,\Omega_r))\;/} \end{cases} \quad (13)$$

Definition 14: we define a reordering function (see Figure 8)

$$\alpha(K) := ((K - 2^{\lfloor \frac{\text{Log}K}{\text{Log}2} \rfloor - 1} + 5 * 2^{\lfloor \frac{\text{Log}K}{\text{Log}2} \rfloor - 3})[6 * 2^{\lfloor \frac{\text{Log}K}{\text{Log}2} \rfloor - 3}] - 2^{\lfloor \frac{\text{Log}K}{\text{Log}2} \rfloor - 2})[2^{\lfloor \frac{\text{Log}K}{\text{Log}2} \rfloor}] + 2^{\lfloor \frac{\text{Log}K}{\text{Log}2} \rfloor - 1} \quad (14)$$

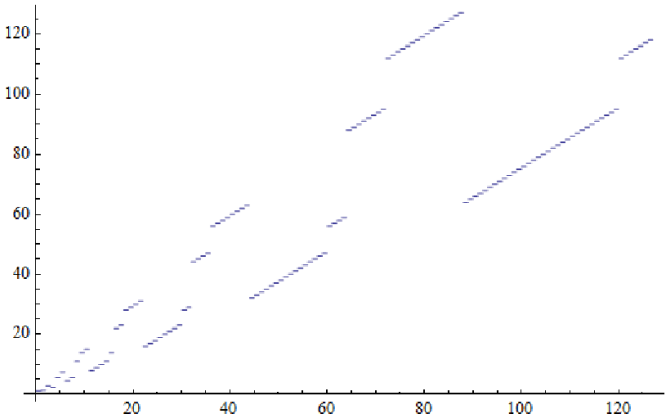

Fig. **8**. Plot of the $\boldsymbol{\alpha}$ (n) function (the values of $\boldsymbol{\alpha}$ versus n).

Table 1. Field values for the 48 leaves of the triple binary tree $\mathbb{T}_7 = \Xi(\mathbb{B}_7)$ based on ${\Omega_6}^\dagger$, pointing toward linked supernode, such that opposite leaves have opposite field.

TABLE I
VALUES OF $\mathbb{E}(n_k)$ FIELD

K	$\{\zeta(K,{\Omega_6}^\dagger)\}$	ω_k	$\{u_k\}$	K	$\{\zeta(K,{\Omega_6}^\dagger)\}$	ω_k	$\{u_k\}$
1	$\{1,0,0,0\}$	0	$\{0,0,0,0\}$	25	$\{-1,0,0,0\}$	$\frac{1}{2}$	$\{0,\frac{1}{2\sqrt{3}},\frac{1}{2\sqrt{3}},\frac{1}{2\sqrt{3}}\}$
2	$\{\frac{1}{\sqrt{2}},\frac{1}{\sqrt{2}},0,0\}$	$\frac{1}{8}$	$\{0,\frac{1}{8},0,0\}$	26	$\{-\frac{1}{\sqrt{2}},-\frac{1}{\sqrt{2}},0,0\}$	$\frac{3}{8}$	$\{0,-\frac{3}{8},0,0\}$
3	$\{0,0,1,0\}$	$\frac{1}{4}$	$\{0,0,\frac{1}{4},0\}$	27	$\{0,0,-1,0\}$	$\frac{1}{4}$	$\{0,0,-\frac{1}{4},0\}$
4	$\{0,0,\frac{1}{\sqrt{2}},-\frac{1}{\sqrt{2}}\}$	$\frac{1}{4}$	$\{0,0,\frac{1}{4\sqrt{2}},-\frac{1}{4\sqrt{2}}\}$	28	$\{0,0,-\frac{1}{\sqrt{2}},\frac{1}{\sqrt{2}}\}$	$\frac{1}{4}$	$\{0,0,-\frac{1}{4\sqrt{2}},\frac{1}{4\sqrt{2}}\}$
5	$\{0,1,0,0\}$	$\frac{1}{4}$	$\{0,\frac{1}{4},0,0\}$	29	$\{0,-1,0,0\}$	$\frac{1}{4}$	$\{0,-\frac{1}{4},0,0\}$
6	$\{-\frac{1}{\sqrt{2}},\frac{1}{\sqrt{2}},0,0\}$	$\frac{3}{8}$	$\{0,\frac{3}{8},0,0\}$	30	$\{\frac{1}{\sqrt{2}},-\frac{1}{\sqrt{2}},0,0\}$	$\frac{1}{8}$	$\{0,-\frac{1}{8},0,0\}$
7	$\{0,0,0,1\}$	$\frac{1}{4}$	$\{0,0,0,\frac{1}{4}\}$	31	$\{0,0,0,-1\}$	$\frac{1}{4}$	$\{0,0,0,-\frac{1}{4}\}$
8	$\{0,0,\frac{1}{\sqrt{2}},\frac{1}{\sqrt{2}}\}$	$\frac{1}{4}$	$\{0,0,\frac{1}{4\sqrt{2}},\frac{1}{4\sqrt{2}}\}$	32	$\{0,0,-\frac{1}{\sqrt{2}},-\frac{1}{\sqrt{2}}\}$	$\frac{1}{4}$	$\{0,0,-\frac{1}{4\sqrt{2}},-\frac{1}{4\sqrt{2}}\}$
9	$\{\frac{1}{2},\frac{1}{2},\frac{1}{2},\frac{1}{2}\}$	$\frac{1}{6}$	$\{0,\frac{1}{6\sqrt{3}},\frac{1}{6\sqrt{3}},\frac{1}{6\sqrt{3}}\}$	49	$\{-\frac{1}{2},-\frac{1}{2},-\frac{1}{2},-\frac{1}{2}\}$	$\frac{1}{3}$	$\{0,-\frac{1}{3\sqrt{3}},-\frac{1}{3\sqrt{3}},-\frac{1}{3\sqrt{3}}\}$
10	$\{0,\frac{1}{\sqrt{2}},\frac{1}{\sqrt{2}},0\}$	$\frac{1}{4}$	$\{0,\frac{1}{4\sqrt{2}},\frac{1}{4\sqrt{2}},0\}$	50	$\{0,-\frac{1}{\sqrt{2}},-\frac{1}{\sqrt{2}},0\}$	$\frac{1}{4}$	$\{0,-\frac{1}{4\sqrt{2}},-\frac{1}{4\sqrt{2}},0\}$
11	$\{-\frac{1}{2},-\frac{1}{2},\frac{1}{2},\frac{1}{2}\}$	$\frac{1}{3}$	$\{0,-\frac{1}{3\sqrt{3}},\frac{1}{3\sqrt{3}},\frac{1}{3\sqrt{3}}\}$	51	$\{\frac{1}{2},\frac{1}{2},-\frac{1}{2},-\frac{1}{2}\}$	$\frac{1}{6}$	$\{0,\frac{1}{6\sqrt{3}},-\frac{1}{6\sqrt{3}},-\frac{1}{6\sqrt{3}}\}$
12	$\{0,-\frac{1}{\sqrt{2}},\frac{1}{\sqrt{2}},0\}$	$\frac{1}{4}$	$\{0,-\frac{1}{4\sqrt{2}},\frac{1}{4\sqrt{2}},0\}$	52	$\{0,\frac{1}{\sqrt{2}},-\frac{1}{\sqrt{2}},0\}$	$\frac{1}{4}$	$\{0,\frac{1}{4\sqrt{2}},-\frac{1}{4\sqrt{2}},0\}$
13	$\{-\frac{1}{2},\frac{1}{2},\frac{1}{2},-\frac{1}{2}\}$	$\frac{1}{3}$	$\{0,\frac{1}{3\sqrt{3}},\frac{1}{3\sqrt{3}},-\frac{1}{3\sqrt{3}}\}$	53	$\{\frac{1}{2},-\frac{1}{2},-\frac{1}{2},\frac{1}{2}\}$	$\frac{1}{6}$	$\{0,-\frac{1}{6\sqrt{3}},-\frac{1}{6\sqrt{3}},\frac{1}{6\sqrt{3}}\}$
14	$\{-\frac{1}{\sqrt{2}},0,0,-\frac{1}{\sqrt{2}}\}$	$\frac{3}{8}$	$\{0,0,0,-\frac{3}{8}\}$	54	$\{\frac{1}{\sqrt{2}},0,0,\frac{1}{\sqrt{2}}\}$	$\frac{1}{8}$	$\{0,0,0,\frac{1}{8}\}$
15	$\{-\frac{1}{2},\frac{1}{2},-\frac{1}{2},\frac{1}{2}\}$	$\frac{1}{3}$	$\{0,\frac{1}{3\sqrt{3}},-\frac{1}{3\sqrt{3}},\frac{1}{3\sqrt{3}}\}$	55	$\{\frac{1}{2},-\frac{1}{2},\frac{1}{2},-\frac{1}{2}\}$	$\frac{1}{6}$	$\{0,-\frac{1}{6\sqrt{3}},\frac{1}{6\sqrt{3}},-\frac{1}{6\sqrt{3}}\}$
16	$\{-\frac{1}{\sqrt{2}},0,0,\frac{1}{\sqrt{2}}\}$	$\frac{3}{8}$	$\{0,0,0,\frac{3}{8}\}$	56	$\{\frac{1}{\sqrt{2}},0,0,-\frac{1}{\sqrt{2}}\}$	$\frac{1}{8}$	$\{0,0,0,-\frac{1}{8}\}$
17	$\{-\frac{1}{2},\frac{1}{2},\frac{1}{2},\frac{1}{2}\}$	$\frac{1}{3}$	$\{0,\frac{1}{3\sqrt{3}},\frac{1}{3\sqrt{3}},\frac{1}{3\sqrt{3}}\}$	57	$\{\frac{1}{2},-\frac{1}{2},-\frac{1}{2},-\frac{1}{2}\}$	$\frac{1}{6}$	$\{0,-\frac{1}{6\sqrt{3}},-\frac{1}{6\sqrt{3}},-\frac{1}{6\sqrt{3}}\}$
18	$\{-\frac{1}{\sqrt{2}},0,\frac{1}{\sqrt{2}},0\}$	$\frac{3}{8}$	$\{0,0,\frac{3}{8},0\}$	58	$\{\frac{1}{\sqrt{2}},0,-\frac{1}{\sqrt{2}},0\}$	$\frac{1}{8}$	$\{0,0,-\frac{1}{8},0\}$
19	$\{-\frac{1}{2},-\frac{1}{2},\frac{1}{2},\frac{1}{2}\}$	$\frac{1}{3}$	$\{0,-\frac{1}{3\sqrt{3}},-\frac{1}{3\sqrt{3}},\frac{1}{3\sqrt{3}}\}$	59	$\{\frac{1}{2},\frac{1}{2},\frac{1}{2},-\frac{1}{2}\}$	$\frac{1}{6}$	$\{0,\frac{1}{6\sqrt{3}},\frac{1}{6\sqrt{3}},-\frac{1}{6\sqrt{3}}\}$
20	$\{0,-\frac{1}{\sqrt{2}},0,\frac{1}{\sqrt{2}}\}$	$\frac{1}{4}$	$\{0,-\frac{1}{4\sqrt{2}},0,\frac{1}{4\sqrt{2}}\}$	60	$\{0,\frac{1}{\sqrt{2}},0,-\frac{1}{\sqrt{2}}\}$	$\frac{1}{4}$	$\{0,\frac{1}{4\sqrt{2}},0,-\frac{1}{4\sqrt{2}}\}$
21	$\{-\frac{1}{2},-\frac{1}{2},\frac{1}{2},-\frac{1}{2}\}$	$\frac{1}{3}$	$\{0,-\frac{1}{3\sqrt{3}},\frac{1}{3\sqrt{3}},-\frac{1}{3\sqrt{3}}\}$	61	$\{\frac{1}{2},\frac{1}{2},-\frac{1}{2},\frac{1}{2}\}$	$\frac{1}{6}$	$\{0,\frac{1}{6\sqrt{3}},-\frac{1}{6\sqrt{3}},\frac{1}{6\sqrt{3}}\}$
22	$\{0,-\frac{1}{\sqrt{2}},0,-\frac{1}{\sqrt{2}}\}$	$\frac{1}{4}$	$\{0,-\frac{1}{4\sqrt{2}},0,-\frac{1}{4\sqrt{2}}\}$	62	$\{0,\frac{1}{\sqrt{2}},0,\frac{1}{\sqrt{2}}\}$	$\frac{1}{4}$	$\{0,\frac{1}{4\sqrt{2}},0,\frac{1}{4\sqrt{2}}\}$
23	$\{-\frac{1}{2},\frac{1}{2},-\frac{1}{2},-\frac{1}{2}\}$	$\frac{1}{3}$	$\{0,\frac{1}{3\sqrt{3}},-\frac{1}{3\sqrt{3}},-\frac{1}{3\sqrt{3}}\}$	63	$\{\frac{1}{2},-\frac{1}{2},\frac{1}{2},\frac{1}{2}\}$	$\frac{1}{6}$	$\{0,-\frac{1}{6\sqrt{3}},\frac{1}{6\sqrt{3}},\frac{1}{6\sqrt{3}}\}$
24	$\{-\frac{1}{\sqrt{2}},0,-\frac{1}{\sqrt{2}},0\}$	$\frac{3}{8}$	$\{0,0,-\frac{3}{8},0\}$	64	$\{\frac{1}{\sqrt{2}},0,\frac{1}{\sqrt{2}},0\}$	$\frac{1}{8}$	$\{0,0,\frac{1}{8},0\}$

Definition 15: we define the lattice of connected triple-binary graphs, modulo x_0 (see Figure 7 for $\mathbb{L}(\mathbb{T}_7,\{2,2,2,2\})$)

$$\mathbb{L}(\mathbb{T}_{r+1},x_0):=\mathrm{U}(\mathbb{T}_r(x))\mathrm{UU}(n_k(\mathbb{T}_{r+1}(x)),\underset{n_k\in\mathrm{nodes}(\mathbb{T}_{r+1}),k2^r,k<11*2^{r-3}}{n_{\alpha(k)}}(\mathbb{T}_{r+1}(x+2^{\frac{k[2]}{2}}\exp(\mathbb{E}(n_k(\mathbb{T}_{r+1}(x))))[x_0])))\qquad(15)$$

Definition 16: we define a lattice condition

$$\text{Lattice condition on } \mathbb{E}(\text{therefore on } \Omega_r):\forall n_k\in\mathrm{nodes}(\mathbb{T}_{r+1}),k\ \ 2^r,k<11*2^{r-3},\mathbb{R}^4(2^{\frac{2+k[2]}{2}}\exp(\mathbb{E}(n_k(\mathbb{T}_{r+1}(x)))))\in\mathbb{N}^4\qquad(16)$$

Theorem 1: Lattice condition (16) holds for $\Omega_6{}^{\dagger}$

Demonstration: The values taken by $\mathbb{E}$ on the 48 leaves are the 24 units of the Hurwitz integer, forming the binary tetrahedral group, and their products by (1+i). They are also coordinates of the 24-cell [17] and its dual scaled by square root of two (see Table 1). They form the integer lattice F4, of the roots of Lie Algebra $\mathfrak{f}4$.

A large family of graphiton models can be built by varying r, Ω_r and x_0 , while (16) holds.

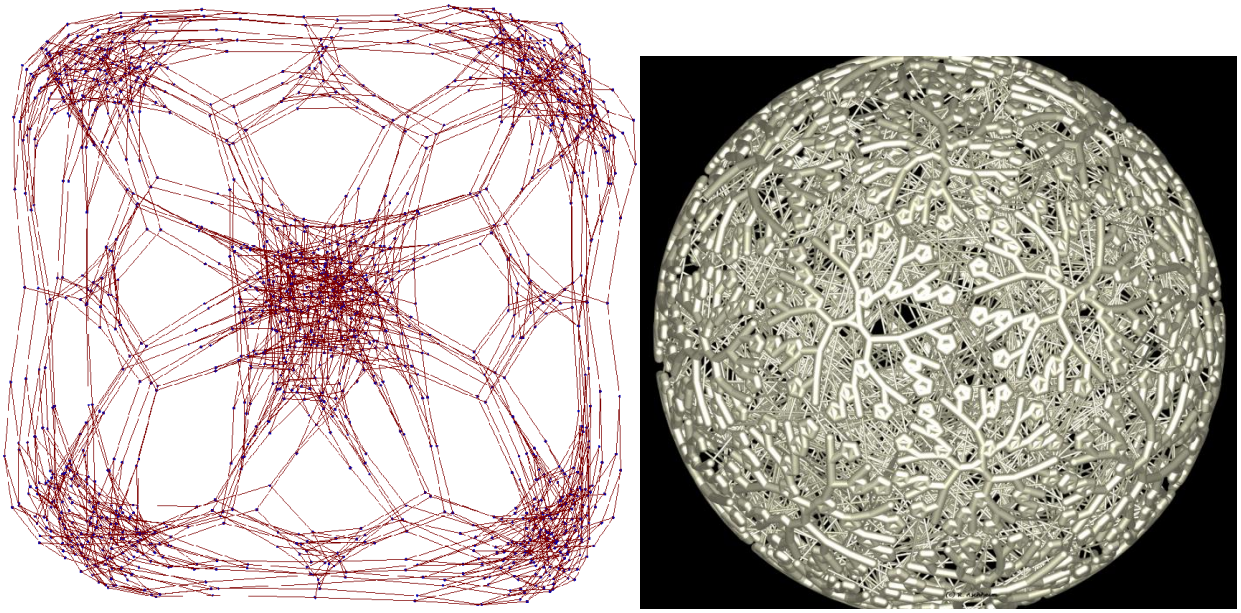

Fig. 9. (a) (left): Level 1 view of second simplest closed lattice of triple binary trees with $\boldsymbol{\Omega_6}^{\dagger}$ is made of 32 modules $\mathbb{T}$ [6] and has 2304 connections (b) (right) An artistic view of the same topology.

III. ENCODING STANDARD MODEL

The idea of encoding particles as topological features in a trivalent network appears in [18], where figure 5 shows a tetrahedron made of 6 connected strings as a model of localized particle.

We define as "Hyperdiamond model" the graphiton model with $\boldsymbol{\Omega}=\boldsymbol{\Omega_6}^{\dagger}$ (see Figure 9). Its intrinsic space is four dimensional, and the 48 valent supernode is perfectly and naturally suited to encode E8 roots according to Lisi's [19] model.

Topological bits in a triple binary tree according to our method preserves the intrinsic geometry. The center of the super node is determined as the single loop of size 4. Associated with the adjacent single triangle they form the central triangle of three nodes respectively informed of bits 0, 0 and 1, and each connected to a first node of binary tree associated respectively with 0, 1 and 1. Thus, each tree root is characterized by a binary code on two different bits, and then the subsequent nodes of the branches at each level are identified by 0 and 1. And the 24 leaves of three binary trees of rank 6 are characterized by a 5-bit identifier (see Figure 10a)

The Lattice condition Equation (16) expresses that the identifiers of two connected leaves issued from two connected triple trees have binary identifiers correlated by the function α which introduces redundant information and thus tolerance to disturbance.

At level 2 the supernode include 21 bits, 3 at the center which are used to characterizes one of the 3 families, and a fermion, boson or photon state, and for the selected family, one pair of triplets of bits encoding a "higgsonic" index and a "gluonic" index.

In this fermion encoding algorithm (see Figure 10b), families are linked by triality and a third of circle rotation,

and matter is related to anti-matter by a space inversion, as in Atiyah's conformal self-dual spaces.[20].

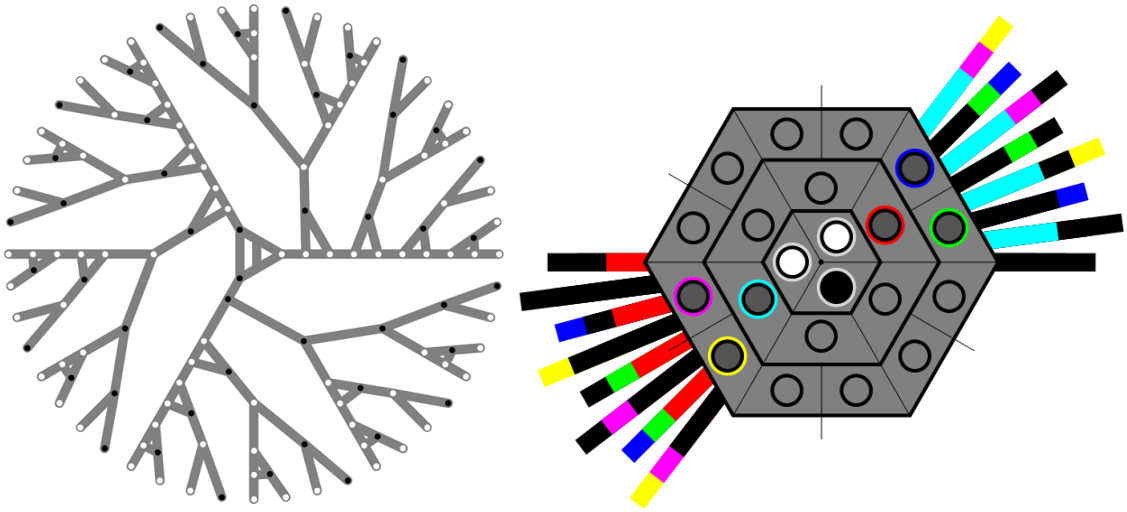

Fig. **10**. . (a) (left): Level 0 structure of a void supernode. (b) (right): Level 2 view of Fermion encoding (for family 1: electron, neutrino, up, down). Other families deduces by rotation of 1/3 or 2/3. Three bits (r,v,b) for gluonic part and three bits (c,m,y) for higgsonic part. Each part has the quaternionic value of attributed direction. Together they form the corresponding E8 root, compatible with Lisi's encoding table.

IV. CONCLUSION

Our hyperdiamond model is the result of hacking reality. A reality emergent from set theory is inherently discrete at ultimate level. Digital is even more pertinent because of the binary encoded content of this proto-space structure. Bit engraving in a topological trivalent network uses the simplest topological feature: a loop. Geometrical level appears by crystallization upon ultimately symmetrical shape of any dimensions: exceptional self-dual regular 24-cell polytope. Quaternion algebra arises naturally. Self-duality gives a non associative double-covering of the F4 lattice where emerges 240 E8 roots. Hacking shows how, from nothing, emerges a really rich notion of void, as a perfect crystal, which defines every known particle, using E8 model [19], in the supernodes, just by internal bit inversion, realized by the most conservative network evolution. Loop quantum gravity formalism [21] can apply to the underlying spin network equipped with implicit frame field. General relativity is achieved through Ashtekar variables [22] and some explicit algorithms like [23] can solve simulations. So the analog world observed at our scale is just a smoothing of a digital nature of the universe at ultimate scale: a beautiful crystal based on the number 24 [24].

References

[1] R. Aschheim, "Bitmaps for a Digital Theory of Everything," presented at the 2008 Midwest NKS conference, Indiana University, Bloomington, IN, Oct. 31–Nov 02, 2008. Available: http://www.cs.indiana.edu/~dgerman/2008midwestNKSconference/rasch.pdf.

[2] R. Aschheim, "From NKS to E8 symmetry, a description of the universe," presented at the JOUAL'09, CNR, Pisa, Italy, Jul 10, 2009.

[3] R. Aschheim, "Graphitation, digital relativity," poster presented at the 2010 NKS Summer School, Vermont Univ., Burlington, VT, Jul 9, 2010

[4] A. Chamseddine, "Noncommutative Geometry as the Key to Unlock the Secrets of Space-Time," Jan 2009. 21pp. Contribution to a special volume in honor of Alain Connes in occasion of his 60th birthday. To be published in the Proceedings series of the Clay Mathematics Institute. Editors E. Blanchard et al. Available: http://arxiv.org/abs/0901.0577.

[5] F. Markopoulou, L. Smolin, "Quantum Theory from Quantum Gravity" in *Phys.Rev. D70 (2004) 124029*. Available: http://arxiv.org/abs/gr-qc/0311059.

[6] T. Konopka, F. Markopoulou, S. Severini, "Quantum Graphity: A Model of emergent locality" in *Phys.Rev. D77:104029,2008*. Available: http://arxiv.org/abs/0801.0861.

[7] G. de Ockam, (Quaestiones et decisiones in quatuor libros Sententiarum cum centilogio theologico, livre II) (1319). Available: http://fondotesis.us.es/fondos/libros/256/553/quaestiones-et-decisiones-in-iv-libros-sententiarum-cum-centilogio-theologico/?desplegar=2708.

[8] G. de Ockam, (Dialogus, part 3, tract 2, book 3, chapter17) (1340),. Available: http://www.britac.ac.uk/pubs/dialogus/t32d3c3.html.

[9] J. W. Alexander; G. B. Briggs, On types of knotted curves. Ann. of Math. (2) 28 (1926/27), no. 1-4, 562--586.

[10] Wolfram, S. *A New Kind of Science*, Champaign, IL: Wolfram Media, 2002.

[11] T. Bolognesi. *Planar trinet dynamics with two rewrite rules*. Complex Systems, 18(1):1{41, 2008., Available: http://www.complex-systems.com/pdf/18-1-1.pdf

[12] J. Ambjørn, J. Jurkiewicz, and R. Loll, "Emergence of a 4D World from Causal Quantum Gravity", Phys. Rev. Lett. 93, 131301 (2004), Available: http://arxiv.org/abs/hep-th/0404156.

[13] R. Aschheim, "Hyperdiamant", presented at the "From the earth to the stars" symposium, Metz, France, Nov 16-22, 2009, Available on DVD, edited by Ars Mathematica.

[14] J.P. Luminet, *L'Univers chiffonné*, Paris, Fayard, 2001.

[15] A. Connes, *Géométrie non commutative*, InterEditions, Paris, 1990

[16] R. Penrose, *The Road to Reality : A Complete Guide to the Laws of the Universe*, Knopf, February 2005.

[17] A. Boole Stott, "Geometrical deduction of semiregular from regular polytopes and space fillings. ", Verhandelingen der Koninklijke Akademie van Wetenschappente Amsterdam, vol. 11 (1910), nr.1, 3–24.

[18] G. t'Hooft, *A Locally Finite Model for Gravity*, Found Phys (2008) 38: 733–757

[19] A. G. Lisi , *An Exceptionally Simple Theory of Everything*, arXiv:0711.0770

[20] M. F. Atiyah, N. J. Hitchin and I. M. Singer, Self-duality in four dimensional Riemannian geometry, Proc. Roy. Soc. London Ser. A 362 (1978) 425-461

[21] C. Rovelli, *Quantum Gravity* CUP.

[22] A. Ashtekar, *New variables for classical and quantum gravity*, Phys. Rev. Lett. 57, 2244 -2247 (1986).

[23] D. Christensen, G. Egan, *An efficient algorithm for the Riemannian 10j symbols*, Class.Quant.Grav. 19 (2002) 1185-1194, Available: http://arxiv.org/abs/ gr-qc/0110045

[24] J. Baez, "*24*", Presented at *The Rankin Lectures*, Glasgow University, Sep. 19, 2008, Avail.: http://math.ucr.edu/home/baez/numbers/24.pdf